First International Symposium on Flutter and its Application, 2016

LOW-SPEED GALLOPING FOR RECTANGULAR CYLINDERS WITH SIDE RATIOS LARGER THAN UNITY

Claudio Mannini[+1], Antonino M. Marra[+2], Tommaso Massai[+3] and Gianni Bartoli[+4]
[+1] CRIACIV/Department of Civil and Environmental Engineering, University of Florence, Italy

The aeroelastic instability starting at low reduced flow speed due to the interference between vortex-induced vibration (VIV) and transverse galloping, which may be called "low-speed galloping", was studied in the wind tunnel in the case of an elastically-supported slender rectangular cylinder with a side ratio of 1.5 and the short side face perpendicular to the smooth flow. The tests were carried out in a wide Scruton number range, starting from low values and increasing it in small steps through eddy-current viscous dampers. This study helped understanding the dynamics of the interaction between the excitation mechanisms of VIV and galloping and clearly highlighted the transition through several regimes of interference. It was found that a high value of the mass-damping parameter is required to completely decouple the ranges of excitation due to vortex-induced vibration and galloping and for the quasi-steady theory to correctly predict the galloping critical wind speed. This conclusion is also relevant from the engineering point of view, as it means that structures and structural elements with ordinary mass-damping properties can exhibit sustained vibrations where they are not predicted by classical theories of vortex-induced vibration and galloping. The modeling of this low-speed galloping was attempt by slightly modifying the wake oscillator model proposed in 1987 by Tamura and Shimada to predict the interference of VIV and galloping in the case of a square-section cylinder. It was found that a proper choice of the coupling parameter between the wake and the mechanical oscillators allows reproducing correctly the main features of the cylinder response. Finally, low-speed galloping can be positively exploited for low-power energy-harvesting systems, in view of the low onset flow speed and the weak dependency on the Scruton number up to medium values of it.

Keyword: galloping, vortex-induced vibration, rectangular cylinder, wind tunnel tests, turbulent flow, analytical model

1. INTRODUCTION

The transverse galloping instability of slender prismatic elements is usually approached with the quasi-steady theory[1-2]. Nevertheless, it is well known that this model can give accurate predictions of the critical threshold and post-critical behavior only for high-reduced flow speed, in particular much higher than the vortex-resonance range. Indeed, when the dissipation capability of the system is small, *i.e.* the so-called Scruton number is relatively low, this requirement cannot be met. Consequently, vortex shedding plays a crucial role in triggering or quenching the instability mechanism, and the behavior of the fluid-structure system can no longer be described by the quasi-steady theory.

A detailed review of transverse galloping of rectangular cylinders with side ratios between 1 and 2 (short side perpendicular to the flow) at low Scruton number is reported in Mannini *et al.*[3]. Therein, the peculiarities of this aeroelastic instability were highlighted and the phenomenon was addressed as interference (or interaction) between vortex-induced vibration (VIV) and galloping. However, it is also reasonable to consider it as a single-degree-of-freedom instability arising at low reduced flow speed, *i.e.* a "low-speed galloping". Now, it is worth reminding that Nakamura and co-workers[4-5] called low-speed galloping the instability observed for rectangular cylinders with side ratios of 0.2 and 0.4 (long side perpendicular to the flow) at low Scruton number,

[+1]claudio.mannini@unifi.it, [+2]antoninomaria.marra@unifi.it, [+3]tmassai@dicea.unifi.it, [+4]gianni.bartoli@unifi.it

slowly building-up spontaneously from rest for flow speeds significantly lower than the vortex resonance velocity. Its range of excitation was found to merge with the vortex-resonance one, where nevertheless the rate of growth of the oscillation from rest is much higher. The distinction between high-speed and low-speed galloping was also outlined by Matsumoto[6]. However, the phenomenon addressed in the present work is clearly different from the one discussed by Nakamura and co-workers.

In this paper, the interference of vortex-induced vibration and galloping in the case of a rectangular cylinder with a side ratio of 1.5 is investigated through wind tunnel tests in smooth flow. This geometry was found to be very prone to this phenomenon[3]. The Scruton number was varied in small steps from low to high values by introducing additional damping into the system by means of eddy-current magnetic damper devices. This study allowed putting in evidence the complicated transition between regimes of interference between VIV and galloping.

In literature, there are only few attempts to model the interference of vortex-induced vibration and galloping, all relying on the linear superposition of unsteady and quasi-steady forces[7-9]. In particular, herein Tamura and Shimada's model[8] was slightly modified for theoretical reasons and then applied to the considered case study.

2. WIND TUNNEL TESTS

The tests were carried out in the open-circuit boundary-layer CRIACIV wind tunnel in Prato, Italy. The facility presents a test chamber 2.42 m wide, 1.60 m high and 11 m long. The free-stream turbulence intensity is below 0.7%.

A plywood sectional model, 986 mm long (L), 116 mm wide (B) and 77 mm deep (D), was used to perform both static and dynamic tests. To enforce bidimensional flow conditions, symmetric rectangular (450 mm × 150 mm × 4 mm) plywood plates were provided at the model ends. The model was placed horizontally in the wind tunnel with the shorter side of the section perpendicular to the flow.

The measurements of the aerodynamic force coefficients at various angles of attack and of the Strouhal number were performed by means of two high-frequency six-components strain-gauges dynamometers placed at the ends of the model.

In the aeroelastic setup, the model was connected through its longitudinal axis-tube to two shear-type steel frames, whose horizontal elements worked as plate-springs (Figure 1(a)). Only the transverse (vertical) displacement was allowed by the two frames due to the very large in-plane bending stiffness of the vertical elements at which the model was connected. The suspension system was sheltered from wind by means of the screens shown in Figure 1(b). The displacements of the model were recorded with two non-contact laser transducers. The viscous damping of the system was increased in small steps through a device based on the electromagnetic induction principle. The dissipation forces produced by the dampers allowed reaching high values of the Scruton number and therefore investigating in details the low-speed galloping instability.

Figure 1: View of the dynamic setup without (left) and with (right) the sheltering system.

3. EXPERIMENTAL RESULTS

The transverse force coefficient as a function of the angle of attack $C_{Fy}(\alpha)$, and in particular its slope in the origin, is of crucial importance for the determination of the galloping behavior of the cylinder with the quasi-steady theory. The convention adopted to express $C_{Fy}(\alpha)$ is shown in Figure 2, while the results of static tests are shown in Figure 3. The force measurements on the fixed cylinder were also used to determine the Strouhal number $St = n_s D/V = 0.106$, where V denotes the undisturbed flow speed and n_s the frequency of vortex shedding, associated with the dominant peak in the lift coefficient spectrum.

During the dynamic tests, the elastically suspended model was let free to vibrate in the transverse degree of freedom and the flow speed was progressively increased, recording the time history of the displacement. In order to highlight hysteresis phenomena and the presence of multiple stable solutions, measurements were also performed either by reducing the flow speed or by stopping the model and letting the vibrations build up from rest. The complete list of dynamic configurations tested is reported in Table 1. Therein, n_0 and ζ_0 denote respectively the still-air natural frequency of oscillation and the damping ratio. Sc is the Scruton number, defined as follows:

$$Sc = \frac{4\pi M \zeta_0}{\rho B D L} \tag{1}$$

$M = 5.5$ kg being the effective mass of the oscillating system. By defining the reduced flow speed as $U = V/n_0 D$, the Kármán-vortex resonance reduced flow speed is denoted as $U_r = 1/St$, while U_g is the galloping critical reduced flow speed predicted by the quasi-steady theory:

$$U_g = \frac{2Sc}{A_1} \cdot \frac{B}{D} \tag{2}$$

where $A_1 = -dC_{F_y}/d\alpha(0)$. Therefore, it results:

$$\frac{U_g}{U_r} = \frac{2Sc \cdot St}{A_1} \cdot \frac{B}{D} \tag{3}$$

A summary of the results for most of the Scruton number values considered is shown in Figure 4 in terms of $\sqrt{2}$ times the standard deviation of the displacement y' normalized with the cross-flow section dimension D. It is clear that the main excitation of the model starts in the vortex resonance region and the oscillation amplitude increases nearly in a linear way with the flow speed. This trend is kept also for high amplitudes of vibration up to a Scruton number of at least 28, corresponding to an estimated value of U_g/U_r of about 1.6 (see Table 1). By contrast, for $Sc = 37$ and 41 ($U_g/U_r = 2.2$ and 2.4), one can observe a decrease of the amplitude of oscillation for reduced velocities between $1.5U_r$ and $2U_r$ followed by a large jump to a higher branch between $2.5U_r$ and $3U_r$. For even higher Scruton numbers ($Sc = 46$ and 52, corresponding to $U_g/U_r = 2.7$ and 3.0), around $U/U_r = 1.5$ the oscillation amplitude decreases down to a low but non-null value, showing quite irregular time histories.

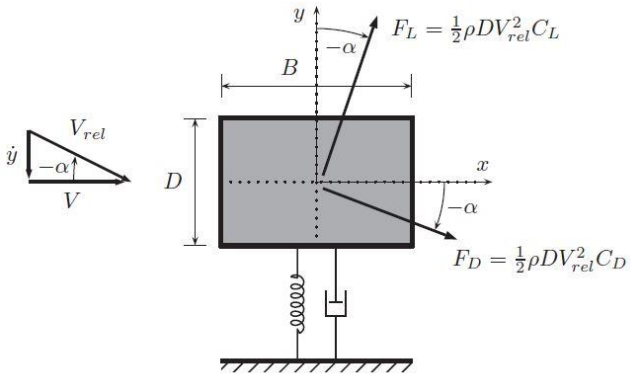

Figure 2: Evaluation of the transverse force on a vibrating rectangular cylinder with the quasi-steady approach. F_D and F_L denote respectively the drag and lift forces per unit length; V_{rel} is the relative flow speed.

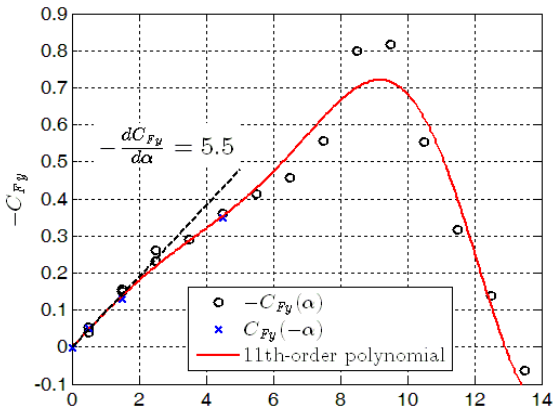

Figure 3: Quasi-steady transverse force coefficient measured in the wind tunnel ($Re = VD/\nu$ = 146,800, V being the flow speed and ν the air kinematic viscosity). The coefficient $C_{Fy}(\alpha)$ is referred to the cross-flow section dimension D. The 11th-order polynomial approximation is also shown.

Table 1: Main characteristics of the configurations tested.

#	n_0 [Hz]	ζ_0 [%]	Sc [-]	U_g [-]	U_g/U_r [-]
1	8.97	0.065	4	2.3	0.24
2	8.97	0.087	6	3.1	0.33
3	8.97	0.22	15	8.1	0.85
4	8.95	0.44	28	15.4	1.63
5	8.97	0.57	37	20.3	2.15
6	8.92	0.64	41	22.9	2.42
7	8.89	0.70	46	25.3	2.68
8	8.93	0.79	52	28.5	3.02
9	8.86	0.91	60	32.7	3.46
10	8.87	0.99	65	36.1	3.82
11	8.84	1.31	86	47.8	5.07
12	8.84	1.85	122	66.6	7.06

A progressive boost of the response is then found commencing at a velocity slightly lower than $2.5U_r$. Finally, for the largest values of the mass-damping parameter considered in the figure (Sc = 60, 65 and 86, corresponding to U_g/U_r = 3.5, 3.8 and 5.0), the vibration of the model sharply dies out slightly after the vortex-resonance flow speed and an excitation appears again with a jump at much higher wind velocities.

Figure 5(a) shows a close-up view of the response in the Kármán-vortex resonance region. It is apparent that in all the tests the initial trend of the response is the same but, increasing the Scruton number, the flow speed at which the maximum amplitude is reached progressively decreases.

Figure 5(b) focuses on the self-limited excitation exhibited by the system for very low reduced flow speed and low values of the Scruton number. This secondary excitation, whose onset velocity does not depend on Sc, can be ascribed to the resonance with the impinging leading-edge vortex mechanism[10-11], which in this particular condition overwhelms the usually dominant Kármán vortex-shedding mechanism.

Figure 6 reports the results for high values of the Scruton number according to the universal plot proposed by Parkinson and Smith[2]. The picture suggests that for $Sc \geq 60$ the high reduced flow speed instability of the rectangular cylinder is due to quasi-steady galloping, as the normalized onset velocity does not change appreciably with the Scruton number. By contrast, a non-negligible anticipation of the instability is already found for Sc = 52. It is also worth noting that the first part of the response beyond the critical flow speed predicted by the quasi-steady theory is significantly different from the experimental results.

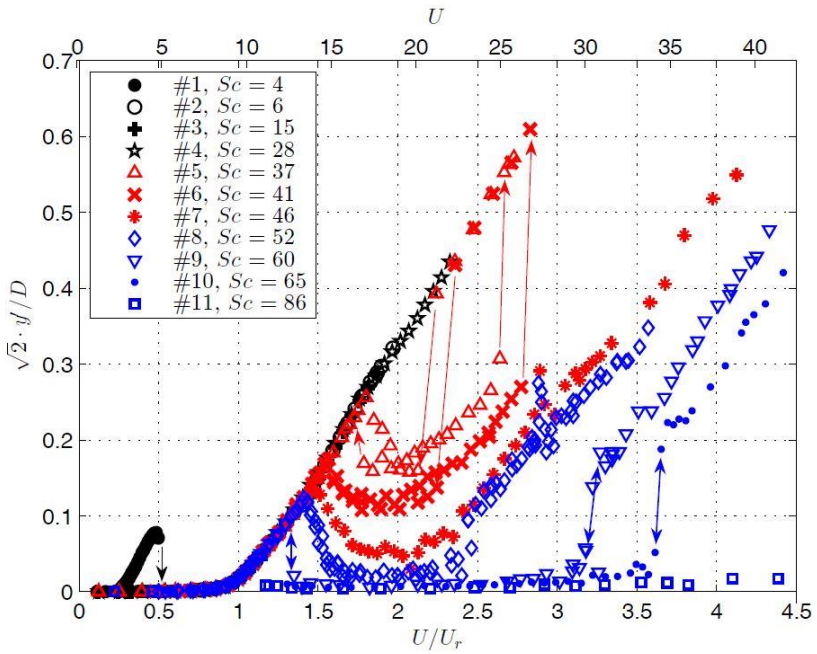

Figure 4: Summary of the amplitude-velocity curves for various Scruton numbers.

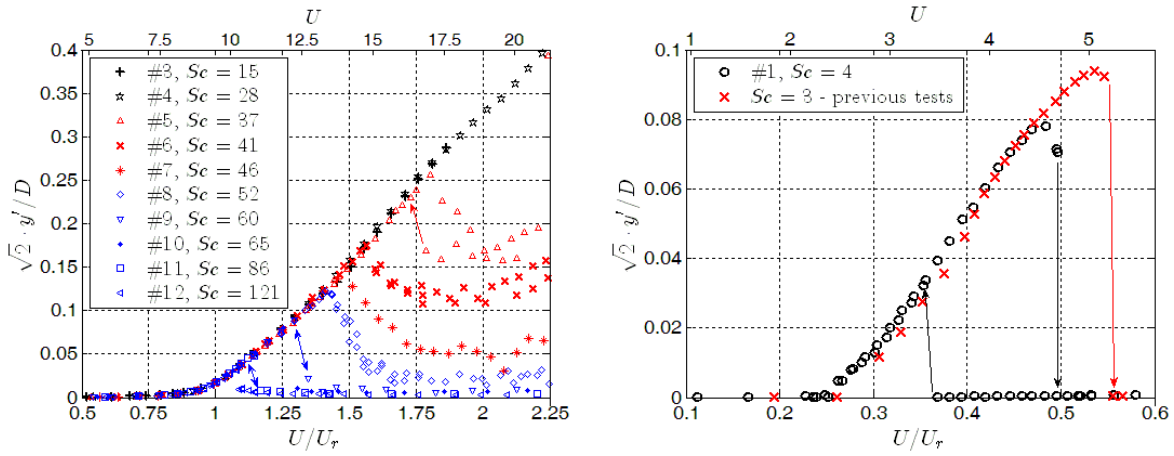

(a) (b)

Figure 5: (a) Amplitude-velocity curves for various Scruton numbers in the Kármán-vortex resonance region; (b) close-up of the response in the low-reduced-flow-speed excitation range for two Scruton numbers.

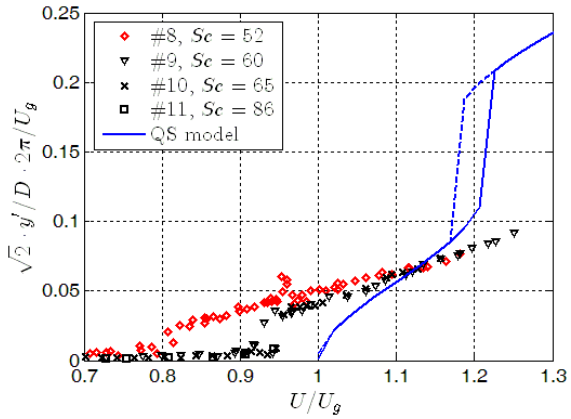

Figure 6: Universal plot of amplitude-velocity curves for high values of the Scruton number.

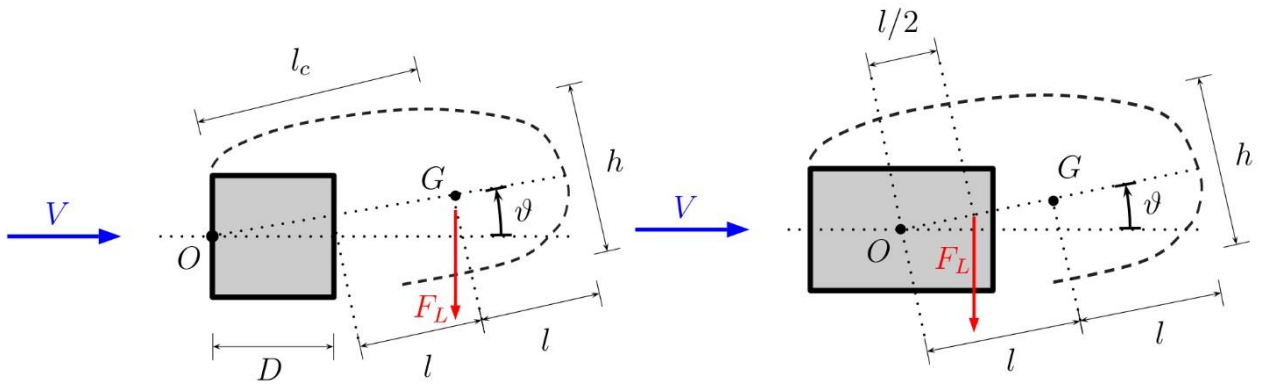

(a) (b)

Figure 7: Schematics of the wake-oscillator model in Tamura and Shimada[8] (a) and in the present work (b).

4. MATHEMATICAL MODEL

In 1987, Tamura and Shimada[8] proposed a model for the interference of VIV and galloping, obtained by simply adding the quasi-steady forces into the wake-oscillator model equations proposed by Tamura and Matsui[12]. The latter was originally conceived to model the vortex-induced vibration of a circular cylinder. It is based on Birkhoff's oscillator model[13] for the dead-air region behind a stationary circular cylinder and it assumes the inclination ϑ of the wake (Figure 7) as time-dependent variable. Funakawa[14] had already linearly coupled Birkhoff's model with a structural oscillator, assuming that the wake oscillator is forced by the body motion (velocity and acceleration) and that the force exerted on the cylinder is proportional to the wake angle ϑ. The resulting linear coefficient f had been determined from experimental tests on a rotating cylinder, in analogy to the Magnus effect[14-15]. Tamura and Matsui[12] included in the wake oscillator model the effect of fluctuation of the length of the dead-air region behind the cylinder as a nonlinear contribution to the stiffness of the restoring spring and the effect of the discharged vortices as an equivalent negative linear damping. Finally, they obtained a Van der Pol equation for the wake angle ϑ. Once the quasi-steady forces have been added, the resulting nonlinear system of differential equations reads:

$$Y'' + 2\zeta_0 Y' + Y = -m^* \frac{U^2}{4\pi^2} f\left(\vartheta + \frac{2\pi Y'}{U}\right) + m^* \frac{U^2}{4\pi^2}\left[A_1 \frac{2\pi Y'}{U} + A_3 \left(\frac{2\pi Y'}{U}\right)^3 + \cdots\right] \tag{4}$$

$$\vartheta'' - 2\beta \upsilon \vartheta' \left(1 - \frac{4f^2}{C_{L0}^2}\vartheta^2\right) + \upsilon^2 \vartheta = -\lambda Y'' - \upsilon^2 \frac{2\pi Y'}{U} \tag{5}$$

where, in addition to the variables previously defined, Y denotes the nondimensional steady-state amplitude of body oscillation (normalized with the cross-flow section dimension D); $\upsilon = St \cdot U = U/U_r$ is the ratio of the flow speed to the vortex resonance velocity (or, alternatively, the ratio of the vortex-shedding frequency to the body natural frequency); $m^* = \rho D^2 L/2M$ is the mass ratio; C_{L0} is the amplitude of lift fluctuation at the Strouhal frequency measured in the wind tunnel for the stationary cylinder; $A_1, A_3, \cdots$ are the coefficients of the polynomial approximation of the quasi-steady transverse force coefficient (Section 3); the prime denotes the derivative with respect to the nondimensional time $\tau = 2\pi n_0 t$.

Herein, Tamura and Shimada's model was slightly modified to account for a pair of inconsistencies introduced by Funakawa[14] with respect to original Birkhoff's model[13] while coupling it with the mechanical oscillator. The difference between the present formulation and Tamura and Shimada's one is schematized in Figure 7 and it implies a different definition of the coefficients β, λ and l^* in Equations (4)-(5):

$$\beta = \frac{f}{\sqrt{2}\pi^2 l^*} \tag{6}$$

$$\lambda = \frac{1}{l^*} \tag{7}$$

$$l^* = \frac{1}{8\pi St^2 h^*} \tag{8}$$

where $h^* = h/D$ is the nondimensional width of the wake.

5. NUMERICAL RESULTS

The 2nd-order differential equations of Tamura and Shimada's model were numerically solved by means of ODE45 Matlab® function. Some control parameters, such as relative and absolute tolerances, have been properly tuned beforehand, so to optimize the accuracy of the solution. To highlight possible hysteresis loops in the solutions, initial condition on the normalized amplitude $Y(0)$ was chosen first equal to 0.01 and then to about the maximum value compatibly with the considered reduced flow speed and the available experimental $C_{Fy}(\alpha)$ data, *i.e.* $Y(0) = 15°\cdot\pi/180\cdot U/2\pi$.

In their analysis of the square-section cylinder, Tamura and Shimada[8] employed the value of the parameter f determined by Funakawa[14] through the analogy with the Magnus effect for the circular cylinder, that is $f = 1.16$. In the authors' opinion, this analogy is questionable, especially for a sharp-edged body and, in any case, the experimental data are not available. Consequently, the value of f was tuned to obtain the best fit of the experimental data for a high value of the Scruton number ($Sc = 86$), *i.e.* in a pure VIV regime, as shown in Figure 8. By contrast, C_{L0} was set to the value 0.656 measured in the wind tunnel, while it was assumed $h^* = 1.8$, as estimated by Tamura and Shimada[8] for the square cylinder. It is apparent in Figure 8 that a value of f equal to 9.28, *i.e.* eight times the reference value of 1.16, gives a very good agreement with the experimental data, except for the hysteresis loop, which was not observed in the experiments. In fact, the analytical model correctly predicts the slope of the amplitude-velocity curve, the peak amplitude and the velocity range of excitation.

Figure 9 shows the same type of analysis for a lower value of the Scruton number ($Sc = 28$, $U_g/U_r = 1.63$), for which a full VIV-galloping interaction was observed in the experiments. For low values of the parameter f either a light interference between the two mechanisms of interference was obtained, with a modest reduction of the galloping critical flow speed (for $f = 0.58$), or the behavior already observed by Tamura and Shimada[8], with the significant overestimation of the response in the resonance region (for $f = 1.16$). By contrast, for higher values of the parameter f, the model is able to predict the nearly linear increase of the response beyond the vortex resonance flow speed observed in the experiments. In particular, if $f = 9.28$ is once again set in the equations, the model's predictions agree reasonably well with the experimental results. It is worth noting that the behavior of the model for such a high value of the coupling parameter has never been explored and therefore the actual potentiality of the model was not clear so far.

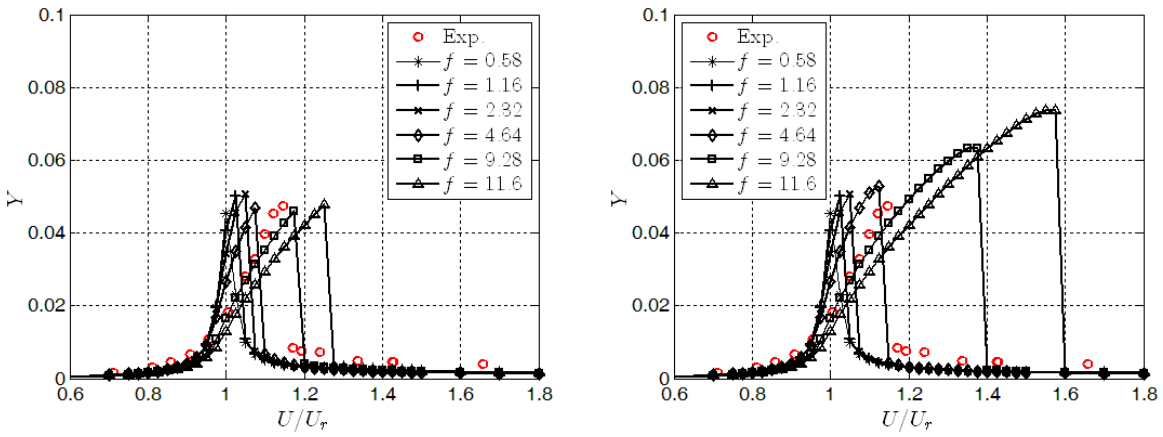

(a) (b)

Figure 8: Comparison between the rectangular cylinder response predicted by the analytical model varying the value of the parameter f and the experimental data for a high value of the Scruton number ($Sc = 86$, test case #11). Numerical results obtained for an initial condition $Y(0) = 0.01$ (a) and $Y(0) = 15°\cdot\pi/180\cdot U/2\pi$ (b).

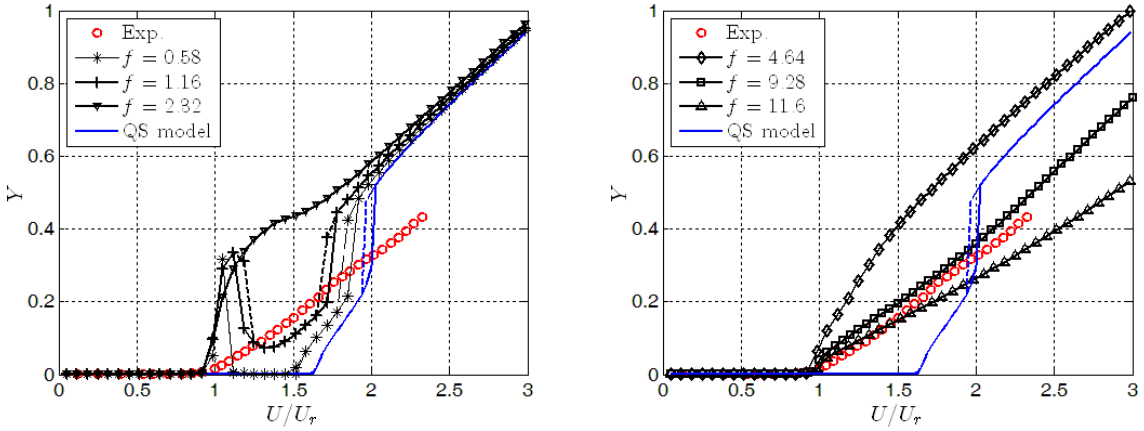

Figure 9: Comparison between the analytical model results obtained varying the value of the parameter f and the experimental data for a value of the Scruton number Sc = 28 (test case #4).

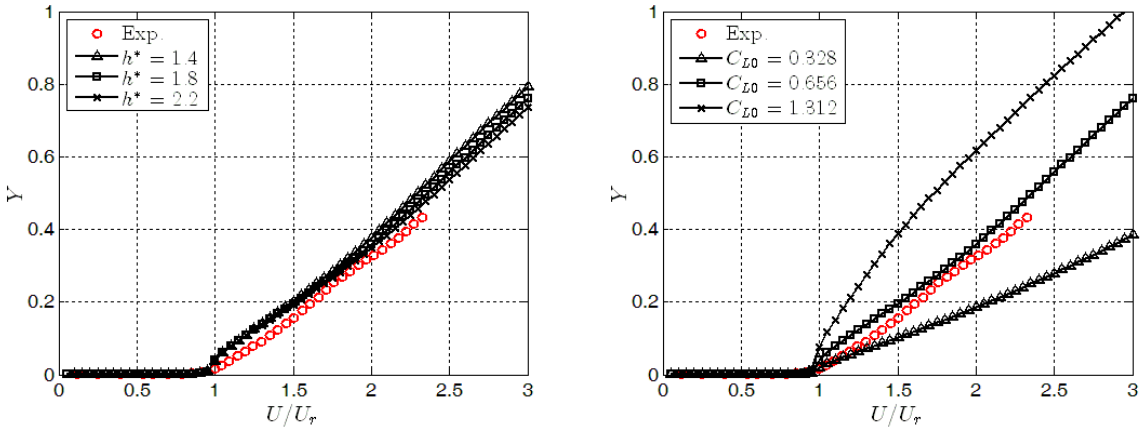

(a) (b)

Figure 10: Sensitivity of the analytical model results (Sc = 28, test case #4, setting f = 9.28) to the variation of the value of the parameter h^* (a) and C_{L0} (b).

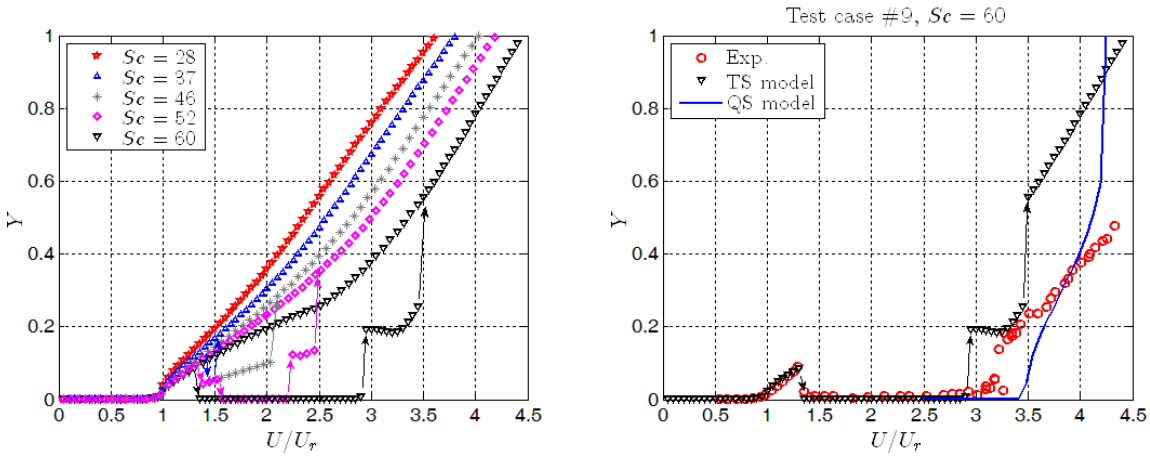

(a) (b)

Figure 11: Amplitude-velocity curves obtained with the analytical model (obtained setting f = 9.28) in the transitional Scruton number range (a) and comparison with experimental results for Sc = 60 (test case #9), considering, for the sake of clarity, only the results relative to the initial condition $Y(0)$ = 0.01 (b).

Figure 10 reports the results of the sensitivity study relative to the parameters h^* and C_{L0}. The former is difficult to be determined, as it requires clear flow visualizations or complicated flow velocity measurements, but it is clear that the results are only weakly dependent on its value in the range of interest. By contrast, the solution of the equations is very sensitive to the value of C_{L0} but this parameter can be easily determined through force measurements on the stationary cylinder, although its value is often uncertain. It is interesting to note that in the investigated range of values, an increase of C_{L0} produces the same effect as a proper reduction of f.

Figure 11(a) shows the amplitude-velocity curves predicted by the analytical model in the range of Scruton number wherein transition occurs between various regimes of interaction of vortex-induced vibration and galloping (see Figure 4). The analytical model predicts no discontinuity between VIV and galloping ranges of excitation for Sc = 37, although a hysteresis loop appears in a very limited range of reduced flow speed (around U/U_r = 1.5). The velocity range of the low-amplitude solution (observed in a similar way also in the experiments, see Figure 4) significantly extends for Sc = 46. By contrast, for Sc = 52 two hysteresis loops are detected and, for reduced flow speeds approximately in the range $1.5 < U/U_r < 2.2$, the cylinder does not vibrate unless a large initial condition is imposed. Finally, for Sc = 60, this intermediate range of stability extends to the left and above all to the right and the hysteresis loop close to the resonance region disappears. In particular, Figure 11(b) compares the numerical results obtained for the initial condition $Y(0) = 0.01$ to experiments for Sc = 60, showing reasonable agreement, despite a slight underestimation of the galloping instability threshold. The discrepancy observed for $U/U_r > 3.5$, where the model solution jumps up to a higher branch, is probably due to the inaccurate polynomial approximation of the experimental transverse force coefficient in the zone of the inflection points, which are known to relate to the hysteresis loop in the amplitude-velocity curve[16].

In general, the analytical model captures the main features of VIV-galloping interference but, as compared to experiments, it tends to overestimate the degree of coupling between the two mechanisms of excitation in the intermediate Scruton number range. In addition, the calculated amplitude-velocity curve reduces the slope by increasing the Scruton number, whereas this does not occur in the experiments.

6. CONCLUDING REMARKS

This paper aims at clarifying the phenomenon of interference between vortex-induced vibration and galloping, called here “low-speed galloping”, for a rectangular cylinder with a side ratio of 1.5. First, a wide experimental campaign in the wind tunnel was carried out, reliably changing the mechanical damping of the system in small steps, so to highlight the transition between various levels of VIV-galloping interference.

High values of the Scruton number, say between 50 and 60 (normalized with the cross-section area), are needed to completely decouple the ranges of excitation due to vortex-induced vibration and galloping. This conclusion has an important impact on the engineering practice, since wind-exposed structures can easily be characterized by lower values of the Scruton number. Therefore, sustained vibrations can be encountered where they are not predicted by codes and standards or classical theories of vortex-induced vibration and galloping. These results can also be read in terms of limits of validity of the quasi-steady theory. In fact, the latter correctly predicts the galloping critical flow speed only for Scruton numbers no lower than about 60, *i.e.* for a ratio of the quasi-steady galloping to the vortex resonance critical flow speed no lower than about 3.5.

From both the scientific and the engineering points of view, it is interesting to understand how the aeroelastic behavior of the cylinder modifies due to oncoming turbulence. With this aim, wind tunnel tests in homogeneous turbulent flows are presently underway. One may already conclude that a low incoming turbulence (intensity of about 3%) seems to promote the mechanism of interference between VIV and galloping for intermediate values of the Scruton number (around 40). This result is in line with the findings of Parkinson and co-workers[17-18] and Bearman[19] for the square section and a higher turbulence intensity (from 7% to 10%).

In this work, the modeling of low-speed galloping was also attempted through a slight modification of Tamura and Shimada’s model. It was concluded that this wake-oscillator model, which also incorporates the quasi-steady force contribution, is able to reproduce the main features of the instability promoted by the interference of VIV and galloping, provided that a proper value of the coupling parameter f is set in the equations. This value is much higher than those ever tested in previous modeling efforts.

Finally, it is worth noting that the interference of vortex-induced vibration and galloping can be positively exploited for low-power energy-harvesting systems. In fact, as compared to pure galloping instability[20], this phenomenon ensures higher levels of power extraction at low wind speed and therefore improved efficiency, as a consequence of the low onset flow speed and the weak dependency on the Scruton number up to medium values of it.

ACKNOWLEDGMENT

The authors wish to thank Luca Pigolotti for the valuable contribution in the development of the experimental setup.

REFERENCES

1) Parkinson G. V., Brooks N. P. H.: On the aeroelastic instability of bluff cylinders, *J. Appl. Mech.*, Vol. 28, pp. 252-258, 1961.
2) Parkinson G. V., Smith J. D.: The square prism as an aeroelastic non-linear oscillator, *Q. J. Mech. Appl. Math.*, Vol. 17, pp. 225-239, 1964.
3) Mannini C., Marra A. M., Bartoli G.: VIV-galloping instability of rectangular cylinders: Review and new experiments, *J. Wind Eng. Ind. Aerodyn.*, Vol. 132, pp. 109-124, 2014.
4) Nakamura Y., Matsukawa T.: Vortex excitation of rectangular cylinders with a long side normal to the flow, *J. Fluid Mech.*, Vol. 180, pp. 171-181, 1987.
5) Nakamura Y., Hirata K.: Pressure fluctuations on oscillating rectangular cylinders with the long side normal to the flow, *J. Fluids Struct.*, Vol. 5, pp. 165-183, 1991.
6) Matsumoto M.: Aerodynamic damping of prisms, *J. Wind Eng. Ind. Aerodyn.*, Vol. 59, pp. 159-175, 1996.
7) Santosham T. V.: *Force measurements on bluff cylinders and aeroelastic galloping of a rectangular cylinder*, Master's thesis, University of British Columbia, Vancouver, Canada, 1966.
8) Tamura Y., Shimada K.: A mathematical model for the transverse oscillations of square cylinders, *Proc. First International Conference on Flow Induced Vibrations*, Bownesson-Windermere, UK, 12-14 May 1987, pp. 267-276, 1987.
9) Corless R. M., Parkinson G. V.: A model of the combined effects of vortex-induced oscillation and galloping, *J. Fluids Struct.*, Vol. 2, pp. 202-220, 1988.
10) Shiraishi N., Matsumoto M.: On classification of vortex-induced oscillation and its application for bridge structures, *J. Wind Eng. Ind. Aerodyn.*, Vol. 14, pp. 419-430, 1983.
11) Naudascher E., Wang Y.: Flow-induced vibrations of prismatic bodies and grids of prisms, *J. Fluids Struct.*, Vol. 7, pp. 341-373, 1993.
12) Tamura Y., Matsui G.: Wake-oscillator model of vortex-induced oscillation of circular cylinder, *Proc. Fifth International Conference on Wind Engineering*, Forth Collins, US, 8-14 July 1979, pp. 1085-1094, 1979.
13) Birkhoff G.: Formation of vortex streets, *J. Appl. Phys.*, Vol. 24, pp. 98-103, 1953.
14) Funakawa M.: The vibration of a cylinder caused by wake force in a flow, *Bull. Japan Soc. Mech. Eng.*, Vol. 12, pp. 1003-1010, 1969.
15) Marris A. W.: A review on vortex streets, periodic wakes, and induced vibration phenomena, *J. Basic Eng.-T. ASME*, Vol. 86, pp. 185-193, 1964.
16) Barrero-Gil A., Sanz-Andres A., Alonso G.: Hysteresis in transverse galloping: The role of inflection points, *J. Fluids Struct.*, Vol. 25, pp. 1007-1020, 2009.
17) Parkinson G. V., Sullivan P. P.: Galloping response of towers, *J. Ind. Aerodyn.*, Vol. 4, pp. 253-260, 1979.
18) Parkinson G. V., Wawzonek M. A.: Some considerations of combined effects of galloping and vortex resonance, *J. Wind Eng. Ind. Aerodyn.*, Vol. 8, pp. 135-143, 1981.
19) Bearman P. W., Gartshore I. S., Maull D. J., Parkinson G. V.: Experiments on fluid-induced vibration of a square-section cylinder, *J. Fluids Struct.*, Vol. 1, pp. 19-34, 1987.
20) Barrero-Gil A., Alonso G., Sanz-Andres A.: Energy harvesting from transverse galloping, *J. Sound Vib.*, Vol. 329, pp. 2873-2883, 2010.